Accepted Manuscript

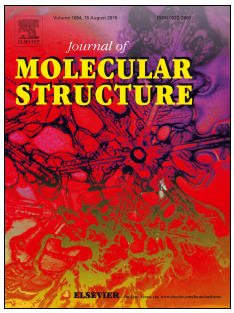

Efficiency of $NaHSO_4$ modified periodic mesoporous organosilica magnetic nanoparticles as a new magnetically separable nanocatalyst in the synthesis of [1,2,4]triazolo quinazolinone/pyrimidine derivatives

Mahdieh Haghighat, Farhad Shirini, Mostafa Golshekan

PII: S0022-2860(18)30699-9

DOI: 10.1016/j.molstruc.2018.05.112

Reference: MOLSTR 25285

To appear in: *Journal of Molecular Structure*

Received Date: 24 February 2018

Revised Date: 29 May 2018

Accepted Date: 31 May 2018

Please cite this article as: M. Haghighat, F. Shirini, M. Golshekan, Efficiency of $NaHSO_4$ modified periodic mesoporous organosilica magnetic nanoparticles as a new magnetically separable nanocatalyst in the synthesis of [1,2,4]triazolo quinazolinone/pyrimidine derivatives, *Journal of Molecular Structure* (2018), doi: 10.1016/j.molstruc.2018.05.112.

Graphical Abstract

Efficiency of $NaHSO_4$ modified periodic mesoporous organosilica magnetic nanoparticles as a new magnetically separable nanocatalyst in the synthesis of [1,2,4]triazolo quinazolinone/pyrimidine derivatives.

Mahdieh Haghighat [a], Farhad Shirini [a,*], Mostafa Golshekan [b]

[a] *Department of Chemistry, College of Sciences, University of Guilan, Rasht, 41335-19141, Iran*

[b] *Institute of Medical Advanced Technologies, Guilan University of Medical Science, Rasht,41346-45971, Iran*

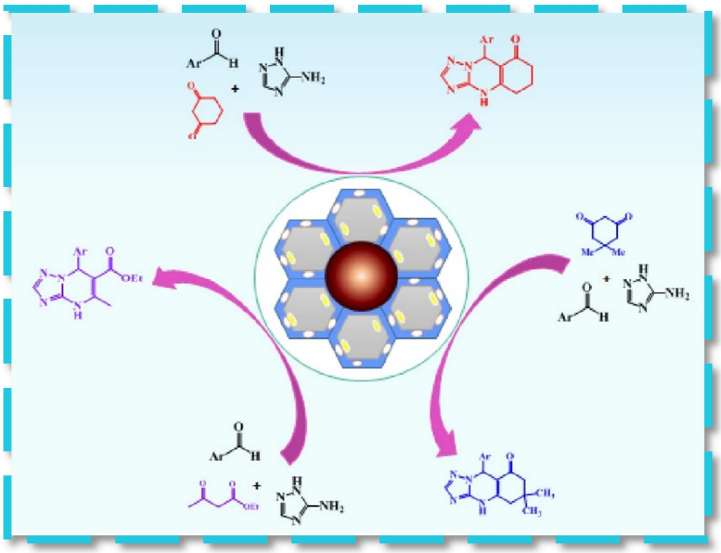

γ-Fe_2O_3@Ph-PMO-$NaHSO_4$ as a new magnetically separable solid acid nanocatalyst is prepared and applied for the synthesis of [1,2,4]triazolo quinazolinone/pyrimidine derivatives.

Efficiency of $NaHSO_4$ modified periodic mesoporous organosilica magnetic nanoparticles as a new magnetically separable nanocatalyst in the synthesis of [1,2,4]triazolo quinazolinone/pyrimidine derivatives

Mahdieh Haghighat[a], Farhad Shirini[a]*, Mostafa Golshekan[b]

[a] *Department of Chemistry, College of Science, University of Guilan, Rasht, 41335-19141, Iran, Tel/Fax: +981313233262; e-mail: shirini@guilan.ac.ir (and also fshirini@gmail.com).*

[b] *Institute of Medical Advanced Technologies, Guilan University of Medical Science, Rasht,41346-45971, Iran*

Abstract— Immobilized $NaHSO_4$ on core/shell phenylene bridged Periodic mesoporous organosilica magnetic nanoparticles (γ-Fe_2O_3@Ph-PMO-$NaHSO_4$) as a new acidic magnetically separable nanocatalyst was successfully prepared in three steps: (i) preparation of γ-Fe_2O_3 nanoparticles by a precipitation method, (ii) synthesis of an organic-inorganic periodic mesoporous organosilica structure with phenyl groups on the surface of γ-Fe_2O_3 magnetic nanoparticles (MNPs) and (iii) finally adsorption of $NaHSO_4$ on periodic mesoporous organosilica (PMO) network. The results of N_2 adsorption-desorption isotherms, XRD and TEM showed formation of the Periodic mesoporous organosilica magnetic nanocomposite with the uniform size up to 15 nm. The efficiency of the new catalyst was evaluated in promoting the synthesis of [1,2,4]triazolo quinazolinone/pyrimidine derivatives as important biologically active compounds. Eco-friendly protocol, high yields, short reaction times, reusability of the catalyst and easy and quick isolation of the products are the main advantages of this procedure.

Keywords: PMO, nanocatalyst; [1,2,4]triazolo quinazolinone, γ-Fe_2O_3@Ph-PMO-$NaHSO_4$.

1. Introduction

Multi-component reactions are one of the most attractive and favourite areas from chemists point of view and play a major role in organic chemistry and pharmaceutical industry because of their significant advantages including feasibility of one-pot synthesis which avoids the extra cost of sequential separation and purification process of the synthetic intermediates, high yields compared with multi-step reactions, better selectivity, short reaction times and experimental cost. Generally, multi-component reactions (MCRs) define as chemical processes which in them more than two substrates condense to provide a product and they are notably perfect and eco-friendly reaction system in the synthesis of condensed heterocycle molecules [1-3].

Synthesis of quinazolinones derivatives as nitrogen-containing heterocycles has drawn a huge consideration because of their biological activities, various applications in pharmaceutical industries and their important role in research and industry [4-12]. Antifungal Epoxiconazole, fluconazole, and albaconazole are examples of some biologically active compounds because of the presence of this group of materials in their structure (see part III in the Supplimentary material) [13-14]. Hence, there is a growing demand for the efficient synthetic ways to make the substituted triazolo quinazolinones. In this way the most common strategy is the reaction of 3-amino-1,2,4-triazole as amine source with various aldehydes and dimedone under different conditions which have been reported in the literature such as MW radiation [15-16], refluxing in DMF [17-18] or in the presence of a variety of promotors including $H_6P_2W_{18}O_{62}$ [19], NH_2SO_3H [20], 1-*n*-butyl-3-methylimidazolium tetrafluoroborate ([Bmim]BF_4) [21], *p*-toluenesulfonic acid [22], acetic acid [23], nano-SiO_2 [24], and sulfonic acid functionalized nanoporous silica (SBA-Pr-SO_3H) [25]. Despite undeniable advantages of these methods, many of them suffer from some drawbacks such as the use of expensive and hazardous

catalysts [19, 24] or solvents [17, 18, 15], harsh conditions [17,18], long reaction times [18] and low yields [17,18]. Now at this time, it is important to develop a more efficient method for the synthesis of triazolo quinazolinones using new catalysts which follows green chemistry principles. It can be achieved by the preparation of nanocatalysts which possesses both properties of homogeneous and heterogeneous systems including high activity and selectivity and easy separation and recovery.

In recent years, porous materials have played a very important role in science and industry so that billion dollars are spent annually in the use of these materials in various fields. Some of these important fields are ionic exchange, separation, catalysis, preparation of batteries, fuel cells, sensors and many others. Among these materials, mesoporous silica has attracted considerable attention in the field of adsorption and catalysis because of its uniform pore size, large pore volume and high surface area [26]. Periodic mesoporous organosilica materials as a member of this family, are a class of hybrid materials which organic groups are distributed in uniformly inside the framework, causing properties including mechanical and hydrothermal stability, diffusion of guest molecule and lack of pore blocking and they are more hydrophobic and stable in water than pure organized silicas (MCM-41 or SBA-15). This feature expands the range of applications in, for example, optical gas sensing, catalysis, chromatography, separation and nanotechnology [27-28]. For the preparation of this kind of materials, a common method included the hydrolysis and condensation of a bridged organosilane precursor of the type $(R`O)_3$ Si-R-Si$(OR`)_3$ (R` is methyl or ethyl and R is an organic group) in the presence of a structure directing agent can be used. Based on this, one-pot synthesis was used as a method for the preparation of periodic mesoporous organosilica magnetic nanocomposite which is possible by the co-condensation of magnetic nanoparticles and tetraethyl orthosilicate (TEOS) with a bridged organosilane precursor of the type $(R`O)_3$ Si-R-Si$(OR`)_3$ in the presence of a surfactant.

So, the synthesis of nanocatalysts with simultaneous use of magnetic nanoparticles and mesoporous silica materials like periodic mesoporous organosilica with the mentioned properties provide the opportunity to chemists to develop catalysts with high surface area and easy separation which can cover some drawbacks of restricted use of inorganic acid or conventional Lewis acids in organic syntheses which is related to their handling, disposal, recovery and reuse them from the reaction mixture.

In continuation of our ongoing research program on the development of nanocatalysts in organic transformations [29-31] and in order to develop simple, efficient, and mild strategies using reusable solid catalysts, in this study a new magnetically separable solid acid nanocatalyst which possesses both features of homogeneous and heterogeneous systems is prepared and applied to the synthesis of [1,2,4]triazolo quinazolinone/pyrimidine. This strategy involves γ-Fe_2O_3 nanoparticles as the magnetic core coated by Ph-PMO as a thin layer on which $NaHSO_4$ is adsorbed.

2. Experimental

2.*1. Materials*

All chemicals including $FeCl_3.6H_2O$ (cat. No: 103943), $FeCl_2.4H_2O$ (cat. No: 103861), tetraethylorthosilicate (TEOS) (cat. No: 800658), 1,4-bis(triethoxysilyl)benzene (cat. No: 598038), sodium bisulfate monohydrate, Pluronic P-123 (M_n:5800 g.mol^{-1} , cat

no: 435465), NaOH, benzaldehyde derivatives, 1,3-cyclohexanedione, dimedone, ethyl acetoacetate and 3-amino-1,2,4-triazole, were purchased with high purity from Sigma-Aldrich and Merck Chemical Company. The purity of the substrates was assessed by TLC on silica-gel polygram SILG / UV 254 plates.

2.2. Characterization techniques

The crystallinity of the prepared nanocatalyst was determined with an X-PERT High Score X-ray diffraction (PANalitical) and measured with Cu Kα radiations in the range of 0.6–80° (2θ). To characterize the composition of the synthesized nanoparticles, a Perkin-Elmer spectrum BX series in the range of 400–4000 cm^{-1} were employed. The determination of particles size and morphology were performed *via* a Philips transmission electron microscopy (TEM, CM10 HT 100 kV). For measuring melting points, a Büchi B-545 apparatus in open capillary tubes were used. N_2 adsorption-desorption was measured by a BELSORP-mini II instrument at 77 K. Before using the samples, they were degassed for 2 h at 120 °C. The specific surface area of each material was calculated using the Brunauer–Emmett Tellet (BET) method. The EDX characterization of the catalyst was conducted on a field emission scanning electron microscope making by TE-SCAN Company and equipped with energy dispersive X-ray spectrometer operating at 15 kV.

2.3. Preparation of the catalyst

2.3.1 Preparation of γ-Fe_2O_3-MNPs

γ-Fe_2O_3-MNPs were chemically synthesized with a little modification in the methodology already described in the literature [32]. For the synthesis of γ-Fe_2O_3-MNPs, ferric chloride hexahydrate $FeCl_3 \cdot 6H_2O$ (11.0 g, 40.7 mmol) and ferrous chloride tetrahydrate $FeCl_2 \cdot 4H_2O$ (4.0 g, 20.1 mmol) were dissolved in deionized water (250 mL) under nitrogen atmosphere with mechanical stirrer at 85 °C in order to prepare the stock solution of ferrous and ferric chloride. Then the prepared solution was slowly added to 250 mL of a 2 mol L^{-1} ammonia solution heated at 80 °C under argon gas protection and stirred vigorously. During the process, the solution temperature was kept constant at 80 °C and argon gas was purged to prevent the intrusion of oxygen. After completion of the reaction, the obtained precipitate of γ-Fe_2O_3-MNPs was separated from the reaction medium by the magnetic field and then was washed four times with 500 mL double-distilled water. Finally, the obtained γ-Fe_2O_3-MNPs were suspended in 500 mL of degassed deionized water.

. *2.3.2 Preparation of γ-Fe_2O_3@Ph-PMO nanocomposite*

For the synthesis of γ-Fe_2O_3@Ph-PMO, 3.3 g Pluronic p123 (Mn = 5800 g/mol) was dissolved in a mixture of γ-Fe_2O_3 (2 g) and concentrated HCl (0.55 mL) in distilled water (120 mL) under argon gas protection at room temperature. Then, 1,4-bis (triethoxysilyl) benzene (2.3) mL and tetraethoxysilane (1.5 mL) were added simultaneously to the mixture dropwise and stirred for 2 hours at 40 °C. At the end of this process, the magnetic composite was kept at 100 °C for 24 h under static conditions. The resultant solid was filtered, and the template was removed by solvent extraction. For this purpose, the magnetic nanocomposite was

dispersed in acetone and refluxed at 56 °C for 10 h, then washed with distilled water and hot ethanol. This procedure was repeated twice to be sure of removing of the surfactant.

2.3.3 Preparation of γ-Fe_2O_3@ Ph-PMO-$NaHSO_4$ nanocatalyst

Based on the method of Golshekan et al [33], γ-Fe_2O_3@Ph-PMO-$NaHSO_4$ was prepared by adding the synthesized mesoporous γ-Fe_2O_3@Ph-PMO nanoparticles (1.5 g) to an aqueous solution of $NaHSO_4 \cdot H_2O$ (20 mL, 0.7 g, 5 mmol) and the mixture was sonicated at 25 °C for 1 min. In continue, the mixture was stirred for 30 min. Finally, water was removed by decanting and the powder was dried in an oven at 90 °C for 2 h. A brown solid acid formulated as γ-Fe_2O_3@ph-PMO-$NaHSO_4$ was obtained. Schematic preparation of γ-Fe_2O_3@ph-PMO-$NaHSO_4$ is shown in Fig. 1.

2.4. General procedure for the synthesis of triazoloquinazolinone/pyrimidine derivatives

20 mg of γ-Fe_2O_3@Ph-PMO-$NaHSO_4$ was added to a round-bottom flask containing an aromatic aldehyde (1mmol), 3-amino-1,2,4-triazole 2 (1.0 mmol), *β*-diketones (dimedone 3, 1,3-cyclohexadione 4 or ethyl acetoacetate 5) (1.0 mmol) and stirred under solvent-free conditions at 100 °C in certain times. Meanwhile, the progress of the reaction was indicated by TLC (*n*-hexane: ethyl acetate; 7:3). With completing the reaction, 3 ml ethanol was poured and the magnetic nanocomposite was separated in the presence of a magnetic stirring bar; the reaction mixture became clear. The crude product was recrystallized from ethanol to give the pure product. The pure products were characterized by conventional spectroscopic methods. Physical and spectral data for the selected compounds are represented below.

9-(4-Bromophenyl)-5,6,7,9-tetrahydro-[1,2,4]triazolo[5,1-*b*]quinazolin-8(4*H*)-one (7c).

White powder; M.p.: 306-308 (°C); IR (KBr, υ, cm^{-1}) 3429 (N-H), 3129 (CH-arom), 2883 (CH-aliph), 1648 (C=O), 1578 (N-H), 621 (C-Br); ^{1}H NMR (400 MHz, DMSO-d_6): δ (ppm) 1.89-2.01 (2H, m, CH_2), 2.22-2.34 (2H, m, CH_2), 2.61-2.71 (2H, m, CH_2), 6.23 (1H, s, CH), 7.18 (2H, d, J = 8.4 Hz, CH-Ph), 7.49 (2H, d, J = 8.4 Hz, CH-Ph), 7.71 (1H, s, CH-triazole), 11.21 (1H, s, NH); ^{13}C NMR (100 MHz, DMSO-d_6): δ (ppm) 21.1, 26.8, 36.7, 44.4, 57.7, 106.6, 121.3, 129.7, 131.6, 141.3, 147.1, 150.6, 153.2, 193.8; Anal. Calcd for $C_{15}H_{13}BrN_4O$: C, 52.19; H, 3.80; Br, 23.15; N, 16.23; O, 4.63.

9-(2-Nitrophenyl)-5,6,7,9-tetrahydro-[1,2,4]triazolo[5,1-*b*]quinazolin-8(4*H*)-one (7d).

White powder; M.p.: 300-304 (°C); IR (KBr, υ, cm^{-1}) 3444 (N-H), 3213 (CH-arom), 2910 (CH-aliph), 1643 (C=O), 1569 (NO_2), 1357 (NO_2); ^{1}H NMR (400 MHz, DMSO-d_6): δ (ppm) 1.88-1.99 (2H, m, CH_2), 2.17-2.27 (2H, m, CH_2), 2.64-2.67 (2H, m, CH_2), 6.98 (1H, s, CH), 7.30 (1H, d, J = 1.2 Hz, CH-Ph), 7.49 (1H, dt, J_1 = 7.6 Hz, J_2 = 0.8 Hz, CH-Ph), 7.61 (1H, dt, J_1 = 7.6 Hz, J_2 = 1.2 Hz, CH-Ph), 7.73 (1H, s, CH-triazole), 7.86 (1H, dd, J_1 = 8 Hz, J_2 = 1.2 Hz, CH-Ph), 11.32 (1H, s, NH); ^{13}C NMR (100 MHz, DMSO-d_6): δ (ppm) 21.1, 26.8, 36.4, 53.4, 106.19, 124.4, 129.4, 129.8, 133.8, 135.3, 147.2, 149.0, 150.8, 153.7, 193.9; Anal. Calcd for $C_{15}H_{13}N_5O_3$: C, 57.87; H, 4.21; N, 22.50; O, 15.42.

3. Results and discussion

3.1. Characterization of the catalyst

3.1.1. FT-IR analysis

Fig. 2 shows the FT-IR spectra of the synthesized γ-Fe_2O_3@Ph-PMO (before and after removal of the template) and γ-Fe_2O_3@Ph-PMO-$NaHSO_4$ MNPs, respectively. Before removal of the template (Fig. 2a), the FT-IR spectra showed high-intensity peaks for the CH_2 stretching modes located at ~2870 and 2970 cm^{-1} (symmetric and asymmetric), as well as for the CH_2 bending mode at ~1473 cm^{-1} which are related to the surfactant tail. The absence of CH_2 peaks in Fig. 2b, confirms the surfactant removal. The sharp band at 1075 cm^{-1} from Si-O stretching confirms the formation of siloxane bonds. The band at 3435 cm^{-1} is from the Si-OH groups. The bands at ~570 and 430 cm^{-1} are related to the Fe-O vibrations. The sulfonic acid bonds can be observed at ~1200–1250, 1010–1100 and 650 cm^{-1}, which are attributed to the O=S=O asymmetric and symmetric stretching vibrations and S-O stretching vibration of SO_3H groups, respectively. However, in the FT-IR spectra of the synthesized nanoparticles, such bands could not be observed because they are probably overlapped by the bands of SiO_2.

3.1.2. X-ray diffraction (XRD) analysis

Fig. 3 shows the powder X-ray diffraction (XRD) pattern of the synthesized γ-Fe_2O_3@Ph-PMO. The peak at 2 theta near 0.9 in the low-angle XRD pattern (Fig. 3a), corresponding to (100) diffraction, characteristics of the formation of mesoporous material with hexagonal mesostructure [34]. Fig. 3b shows the wide-angle XRD measurements between 2 and 80 degrees 2theta of γ-Fe_2O_3@Ph-PMO. The patterns indicates peaks with 2 theta at 30.06°, 35.67°, 43.47°, 53.83°, 57.36° and 62.96° which is quite identical to pure maghmetite and matched well with the XRD pattern of the standard γ-Fe_2O_3 from Joint Committee on Powder Diffraction Standards (JCPDS No. 39-1346)[35]. The average nanoparticel diameter of γ-Fe_2O_3@Ph-PMO was calculated about 12 nm from the XRD results by Scherrer equation.

3.1.3 BET analysis

The results of N_2 adsorption-desorption isotherms of γ-Fe_2O_3@Ph-PMO and γ-Fe_2O_3@Ph-PMO-$NaHSO_4$ were shown in Fig. 4. From N_2 adsorption-desorption analysis of samples, a type IV BET isotherm for both samples was obtained, as shown in Fig. 4, which is attributed to mesoporous structures [34]. The Brunauer-Emmet-Teller (BET) surface areas and total pore volume of γ-Fe_2O_3@Ph-PMO were 357.83 $m^2.g^{-1}$ and 0.5154 cm^3.g, respectively. The BET surface area and total pore volume of γ-Fe_2O_3@Ph-PMO-$NaHSO_4$ decreased which proves the adsorption of $NaHSO_4$ on the surface and successful synthesis of the nanocatalyst. Table 1 summarizes the structural parameters obtained from N_2 adsorption-desorption.

3.1.4 EDX analysis

The energy-dispersive Xray analysis (EDX) analysis (see part IV in the Supplimentary material) of the catalyst showed the presence of Fe, Si, Na, S, O, and C elements in the expected nanocatalyst.

3.1.5 TEM analysis

Fig. 5 shows TEM image of the synthesized γ-Fe_2O_3@Ph-PMO-$NaHSO_4$. The TEM image revealed that all samples were spherical-like particles. Based on the TEM images, analysis of the γ-Fe_2O_3@Ph-PMO-$NaHSO_4$ surface morphology demonstrated that the aggregation of the particles is uniform and the size of them is up to 15 nm.

3.1.6 H^+ Content determination

The amount of exchangeable H^+ for γ-Fe_2O_3@Ph-PMO and γ-Fe_2O_3@Ph-PMO-$NaHSO_4$ was determined by neutralization titration. For this purpose, 0.02 g γ-Fe_2O_3@Ph-PMO and γ-Fe_2O_3@Ph-PMO-$NaHSO_4$ separately, were dispersed in 10 mL of NaCl solution (0.1 M) and stirred for 30 minutes then the mixture was titrated with NaOH (0.02 M) in the presence of phenolphthalein as indicator. The amounts of acidic protons were found to be 0.2 and 0.8mmol. g^{-1} respectively. This result confirms the synthesis of γ-Fe_2O_3@Ph-PMO-$NaHSO_4$ nanocatalyst and acting it as a solid acid catalyst.

3.2. Catalytic activity

The above mentioned structural analysis results directed us to accept that γ-Fe_2O_3@Ph-PMO-$NaHSO_4$ can be used as an acidic catalyst in organic transformations. In order to stabish this suggestion the promoting ability of this reagent was studied in the preparation of [1,2,4]triazolo quinazolinone/pyrimidine derivatives. To stablish the best reaction conditions, the reaction of 4-chlorobenzaldehyde (1.0 mmol), 3-amino-1,2,4-triazole (1.0 mmol), dimedone (1.0 mmol), was selected as a model. The effect of the amounts of the catalyst, temperature, and solvent for the more efficient conditions by using γ-Fe_2O_3@Ph-PMO-$NaHSO_4$ was investigated and the obtained results were arranged in Table 2. Optimization of the model reaction was performed in different polar (CH_3CN, EtOH, H_2O) and nonpolar (CH_2Cl_2) solvents and under solvent-free conditions. As shown in Table 2, solvent-free conditions is more suitable for the synthesis of 9-(4-chlorophenyl)-6,6-dimethyl-5,6,7,9-tetrahydro-[1,2,4]triazolo[5,1-*b*]quinazolin-8(4*H*)-one. To determine the optimum amount of the catalyst, we performed the reaction using different amounts of the catalyst. It is clarified that 0.02 g γ-Fe_2O_3@Ph-PMO-$NaHSO_4$ can effectively catalyze the reaction and resulted the product in the highest yield. Also, we investigated the efficiency of $NaHSO_4$ and γ-Fe_2O_3@Ph-PMO separately for the model reaction. The compiled outcomes in Table 2 represented that using these materials as catalysts led not to complete the reaction (Entry 13, Table 2) or obtained low yield of the products (Entry12, Table 2). But by using γ-Fe_2O_3@Ph-PMO-$NaHSO_4$, the result became noticeably better. After the selection of the best conditions, as indicated in Scheme 1, a wide range of aromatic aldehydes were reacted with 3-amino-1,2,4-triazole 2 (1.0 mmol), *β*-diketones (dimedone 3, 1,3-cyclohexadione 4 or ethyl acetoacetate 5) (1.0 mmol) in the presence of γ-Fe_2O_3@Ph-PMO-$NaHSO_4$ to generate the requested products and the results were summarized in Table 3. Some products were characterized by IR and NMR spectroscopy data. Melting points are compared with reported values in the literature as shown in Table 3.

It is important to note that the super paramagnetic property of the synthesized nanocatalyst made the separation and reuse of this catalyst very easy. Fig. 6 shows the separation of this nanocatalyst from its aqueous dispersion within a few minutes by simple use of an external magnet.

To demonstrate the worthiness of the prepared catalyst, the results obtained from the synthesis of 9-(4-chlorophenyl)-6,6-dimethyl-5,6,7,9-tetrahydro-[1,2,4]triazolo[5,1-*b*]quinazolin-8(4*H*)-one (6b) (Entry 2, Table 3) using this method is compared with the selected catalysts in Table 4. This comparison shows the effectiveness of the heterogeneous catalyst γ-Fe_2O_3@Ph-PMO-$NaHSO_4$ in increasing of the rate and yield of the reaction. The turnover frequency (TOF) was also calculated and the higher amount of it displays the better performance of the prepared catalyst in comparison with others as shown in Table 4. On the other hand, as we have mentioned previously the presented catalyst can be easily separated using an external magnetic field, and the reaction proceeds under mild conditions.

A suggested mechanism for the studied reactions is shown in Scheme 2. According to this mechanism, the γ-Fe_2O_3@Ph-PMO-$NaHSO_4$ catalyst activates the carbonyl group of the aromatic aldehyde which then condenses with enol (b) to produce the intermediate (c). In continue, the process can be divided into two routes. In route 1, Michael addition reaction of nitrogen number 2 in 3-amino-1, 2, 4-triazolo 2 to intermediate (d) makes intermediate (e). An intra-molecular cyclization in (e) happens and it loses water to produce the desired enamine product 6. On the other hand, in route 2, intermediate (d) is attacked by NH_2 group in 3-amino-1, 2, 4-triazolo 2 and after losing water the process continues *via* intermediate (f) to produce the requested product.

3.3. Reusability of the catalyst

The recovery ability of γ-Fe_2O_3@Ph-PMO-$NaHSO_4$ was measured in the synthesis of 9-(4-chlorophenyl)-6,6-dimethyl-5,6,7,9-tetrahydro-[1,2,4]triazolo[5,1-*b*]quinazolin-8(4*H*)-one (6b), under optimized reaction conditions. After completion of the reaction and separation of the catalyst from the reaction mixture, the catalyst was washed with ethanol, dried in air, and reused with the least change in the reaction time and yield even after five cycles of the synthesis of the product (Fig. 7). The amount of acidic protons for both fresh and the recovered catalyst after fifth run was measured by the neutralization titration. According to this, the amount of acidic protons was changed from 0.8 mmol/g for fresh catalyst to 0.6 mmol/g for the recycled catalyst, whereas this factor was 0.2 mmol/g for γ-Fe_2O_3@Ph-PMO, showing that although washing with water/ethanol leached out a small amount of $NaHSO_4$, due to its high solubility, and the products were obtained in the least change in reaction times and yields

4. Conclusion

In conclusion, γ-Fe_2O_3@Ph-PMO-$NaHSO_4$ as a new nanocatalyst was successfully synthesized and utilized as an efficient catalyst for the preparation of [1,2,4]triazolo quinazolinone derivatives under mild conditions and compared with $NaHSO_4$ and γ-Fe_2O_3@Ph-PMO as catalysts. It turned out that γ-Fe_2O_3@Ph-PMO-$NaHSO_4$ functioned better and conveniently. This catalyst is thermally stable, green, recyclable, easy to prepare. In addition, it can be easily separated from the reaction mixture and recovered up to five times without any significant influence on its activity or the reaction yield.

Acknowledgments

We are thankful to the Research Council of the University of Guilan for the partial support of this research.

References

[1] L. Weber, The Application of Multi-Component Reactions in Drug Discovery, Curr. Med. Chem. 9 (2002) 2085-2093.

[2] C. Hulme, V. Gore, Multi-component Reactions: Emerging Chemistry in Drug Discovery 'From Xylocain to Crixivan, Curr. Med. Chem. 10 (2003) 51-80.

[3] A. Domling, Recent Developments in Isocyanide Based Multicomponent Reactions in Applied Chemistry, chem. Rev. 106 (2006) 17-89.

[4] K. Hemalatha, G. Madhumitha, N. A. Al-Dhabi, M. ValanArasu, Importance of fluorine in 2,3-dihydroquinazolinone and its interaction study with lysozyme, J. Photochem. Photobiol. 162 (2016) 176-188.

[5] K. Hemalatha, G. Madhumitha, Study of binding interaction between anthelmintic 2, 3-dihydroquinazolin-4-ones with bovine serum albumin by spectroscopic methods J. Lumin. 178 (2016) 163-171.

[6] S.M. Roopan, A. Bharathi, J. Palaniraja, K. Anand, R.M. Unexpected regiospecific Michael addition product: synthesis of 5,6-dihydrobenzo[1,7]phenanthrolines, RSC Adv. 5 (2015) 38640-38645.

[7] V. Alagarsamy, U. S. Pathak, Synthesis and antihypertensive activity of novel 3-benzyl-2-substituted-3H-[1, 2, 4] triazolo [5, 1-*b*] quinazolin-9-ones, Bioorg. Med. Chem. 15 (2007) 3457-3462.

[8] V. Alagarsamy, G. Murugananthan, R. Venkateshperumal, Synthesis, analgesic, anti-inflammatory and antibacterial activities of some novel 2-methyl-3-substituted quinazolin-4-(3*H*)-ones, Biol. Pharm. Bull. 26 (2003) 1711-1714.

[9] V. Alagarsamy, Synthesis and pharmacological investigation of some novel 2-methyl-3-(substituted methylamino)-(3*H*)-quinazolin-4-ones as histamine H1-receptor blockers, Pharmazie. 59 (2004) 753-755.

[10] M. L. Gujral, P. N. Saxena, R. P. Kohli, Evaluation of anticonvulsant activity of 2, 3-di-substituted quinazolones: a new class of anticonvulsant drugs, Indian J. Med. Res. 45 (1957) 207-211.

[11] M. J. Hour, L. J. Huang, S. C. Kuo, Y. Xia, K. Bastow, Y. Nakanishi, E. Hamel, K. H. Lee, 6-Alkylamino- and 2,3-Dihydro-3'-methoxy-2-phenyl-4-quinazolinones and Related Compounds: Their Synthesis, Cytotoxicity, and Inhibition of Tubulin Polymerization, J. Med. Chem. 43 (2000) 4479-4487.

[12] V. Alagarsamy, R. Revathi, S. Meena, K. V. Ramaseshu, S. Rajasekaran, E. De Clercq, AntiHIV, antibacterial and antifungal activities of some 2, 3-disubstituted quinazolin-4 (3*H*)-ones, Indian J. Pharm. Sci. 66 (2004) 459-462.

[13] K. C. Liu, M. K. Hu, Guanidine-annelated Heterocycles, VII: Synthesis and Antihypertensive Activity of 2, 10-Dimethyl-5*H*, 10*H*-1, 2, 4-triazolo [5, 1-*b*] quinazolin-5-one, Arch. Pharm. 319 (1986) 188-189.

[14] N.G. Aher, V.S. Pore, N.N. Mishra, A. Kumar, P.K. Shukla, A. Sharma, M.K. Bhat, Synthesis and antifungal activity of 1, 2, 3-triazole containing fluconazole analogues, Bioorg. Med. Chem. Lett. 19 (2009) 759-763.

[15] A. E. Mourad, A. A. Aly, H. H. Farag, E. A. Beshr, Microwave assisted synthesis of triazoloquinazolinones and benzimidazoquinazolinones, Beilstein J. Org. Chem. 3 (2007) 1-4.

[16] G. Krishnamurthy, K. V. Jagannath, Microwave-assisted silica-promoted solvent-free synthesis of triazoloquinazolinone and benzimidazoquinazolinones, J. Chem. Sci. 125 (2013) 807-811.

[17] V. V. Lipson, S. M. Desenko, M. G. Shirobokova, V. V. Borodina, Synthesis of 9-Aryl-6,6-dimethyl-5,6,7,9-tetrahydro-1,2,4-triazolo[5,1-*b*]quinazolin-8(4*H*)ones, Chem. Heterocycl. Compd. 39 (2003) 1213-1217.

[18] V. V. Lipson, S. M. Desenko, V. V. Borodina, M. G. Shirobokova, V. I. Musatov, Russ. Synthesis of partially hydrogenated 1, 2, 4-triazoloquinazolines by condensation of 3, 5-diamino-1, 2, 4-triazole with aromatic aldehydes and dimedone, J. Org. Chem. 41 (2005) 114-119.

[19] M. M. Heravi, L. Ranjbar, F. Derikvand, B. Alimadadi, H. A. Oskooie, F. F. Bamoharram, A three component one-pot procedure for the synthesis of [1,2,4]triazolo/benzimidazolo-quinazolinone derivatives in the presence of $H_6P_2W_{18}O_{62}.18H_2O$ as a green and reusable catalyst, Mol. Divers. 12 (2008) 181-185.

[20] M. M. Heravi, F. Derikvand, L. Ranjbar. Sulfamic Acid–Catalyzed, Three-Component, One-Pot Synthesis of [1,2,4]Triazolo/Benzimidazolo Quinazolinone Derivatives, Synth. Commun. 40 (2010) 677-685.

[21] K. Kumari, D. S. Raghuvanshi, K. N. Singh, An Expeditious Synthesis of Tetrahydro-1,2,4-triazolo[5,1-*b*]quinazolin-8(4*H*)-ones and Dihydro-1,2,4-triazolo[1,5-*a*]pyrimidines, Org. Prep. Proced. Int. 44 (2012) 460-466.

[22] M. R. Mousavi, M. T. Maghsoodlou, Catalytic systems containing p-toluenesulfonic acid monohydrate catalyzed the synthesis of triazoloquinazolinone and benzimidazoquinazolinone derivatives, Monatsh. Chem. 145 (2014) 1967-1973.

[23] M. R. Mousavi, M. T. Maghsoodlou, N. Hazeri, S. M. Habibi‐Khorassani, A simple, economical, and environmentally benign protocol for the synthesis of [1,2,4]triazolo[5,1-*b*]quinazolin-8(4*H*)-one and hexahydro[4,5]benzimidazolo[2,1-*b*]quinazolinone derivatives, J. Iran. Chem. Soc. 12 (2015) 1419-1424.

[24] M. R. Mousavi, M. T. Maghsoodlou, Nano-SiO_2: a green, efficient, and reusable heterogeneous catalyst for the synthesis of quinazolinone derivatives, J. Iran. Chem. Soc. 12 (2015) 743-749.

[25] Gh. M. Ziarani, A. Badiei, Z. Aslani, N. Lashgari, Application of sulfonic acid functionalized nanoporous silica (SBA-Pr-SO_3H) in the green one-pot synthesis of triazoloquinazolinones and benzimidazoquinazolinones, Arab. J. Chem. 8 (2015) 54-61.

[26] S. S. Park, M.S. Moorthy, C. H, Periodic mesoporous organosilica (PMO) for catalytic applications, Korean J. Chem. Eng. 31 (2014) 1707-1719

[27] F. Goethals, B. Meeus, A. Verberckmoes, P. Van der Voort, I. Van Driessche, Hydrophobic high quality ring PMOs with an extremely high stability, J. Mater. Chem. 20 (2010) 1709-1716.

[28] N. Mizoshita, T. Tani, S Inagaki. Syntheses, properties and applications of periodic mesoporous organosilicas prepared from bridged organosilane precursors, Chem. Soc. Rev. 40 (2011) 789-800.

[29] O. Goli‐Jolodar, F. Shirini. An efficient and practical synthesis of benzazolo[2,1-*b*]quinazolinones and triazolo[2,1-*b*]quinazolinones catalyzed by nano-sized NS-C_4(DABCO-$SO_3H)_2$)·4Cl, J. Iran. Chem. Soc. 14 (2017) 2275-2286.

[30] F. Kamali, F. Shirini. Introduction of Fe_3O_4@SiO_2–$ZrCl_2$-MNPs for the efficient promotion of some multi-component reactions under solvent-free conditions, New J. Chem. 41 (2017) 11778-11791.

[31] M. Mashhadinezhad, F. Shirini, M. Mamaghani. Nanoporous Na+-montmorillonite perchloric acid as an efficient heterogeneous catalyst for synthesis of merocyanine dyes based on isoxazolone and barbituric acid, Microporous Mesoporous Mater. 262 (2018) 269-282.

[32] N. Saadatjoo, M. Golshekan, S. Shariati, H. Kefayati and P. Azizi. Organic/inorganic MCM-41 magnetite nanocomposite as a solid acid catalyst for synthesis of benzo [α] xanthenone derivatives, J. Mol. Catal. Chem. 377 (2013) 173-179.

[33] M. Golshekan, S. Shariati, N. Saadatjooa. The synthesis of aminonaphtols and β-amino carbonyls in the presence of a magnetic recyclable Fe_3O_4@ MCM-48–$NaHSO_4$ nano catalyst, RSC Adv. 4 (2014) 16589-16596.

[34] C. P. Moura, C. B. Vidal, A. L. Barros, L. S. Costa, L. C.G. Vasconcellos, F. S. Dias, R. F. Nascimento, Adsorption of BTX (benzene, toluene, o-xylene, and p-xylene) from aqueous solutions by modified periodic mesoporous organosilica, J. Colloid Interface Sci. 363 (2011) 626-634.

[35] M. Aliahmad, N. Nasiri moghaddam, Synthesis of maghemite (γ-Fe_2O_3) nanoparticles by thermal-decomposition of magnetite (Fe_3O_4) nanoparticles, Materials Science-Poland, 31 (2013) 264-268.

[36] R. G. Puligoundla, Sh. Karnakanti, R. Bantu, N. Kommu, S. B. Kondra, L. Nagarapu, A simple, convenient one-pot synthesis of [1, 2, 4] triazolo/benzimidazolo quinazolinone derivatives by using molecular iodine, Tetrahedron Lett. 54 (2013) 2480-2483.

[37] N. Seyyedi, F. Shirini, M, Safarpoor Nikoo Langarudi, S Jashnani, A simple and convenient synthesis of [1,2,4]triazolo/ benzimidazolo quinazolinone and [1,2,4]triazolo[1,5-*a*]pyrimidine derivatives catalyzed by DABCO-based ionic liquids, J. Iran. Chem. Soc. 14 (2017) 1859-1867.

[38] A. Shaabani, E. Farhangi, A. Rahmati, Synthesis of tetrahydrobenzimidazo [1, 2-*b*] quinazolin-1 (2*H*)-one and tetrahydro-1, 2, 4-triazolo [5, 1-*b*] quinazolin-8 (4*H*)-one ring systems under solvent-free conditions, Comb. Chem. High Throughput Screening. 9 (2006) 771-776

[39] M. Kidwai, R. Chauhan, Nafion-H® catalyzed efficient one-pot synthesis of triazolo[5,1-*b*]quinazolinones and triazolo[1,5-*a*]pyrimidines: A green strategy, J. Mol. Catal. A: Chem. 377 (2013) 1-6.

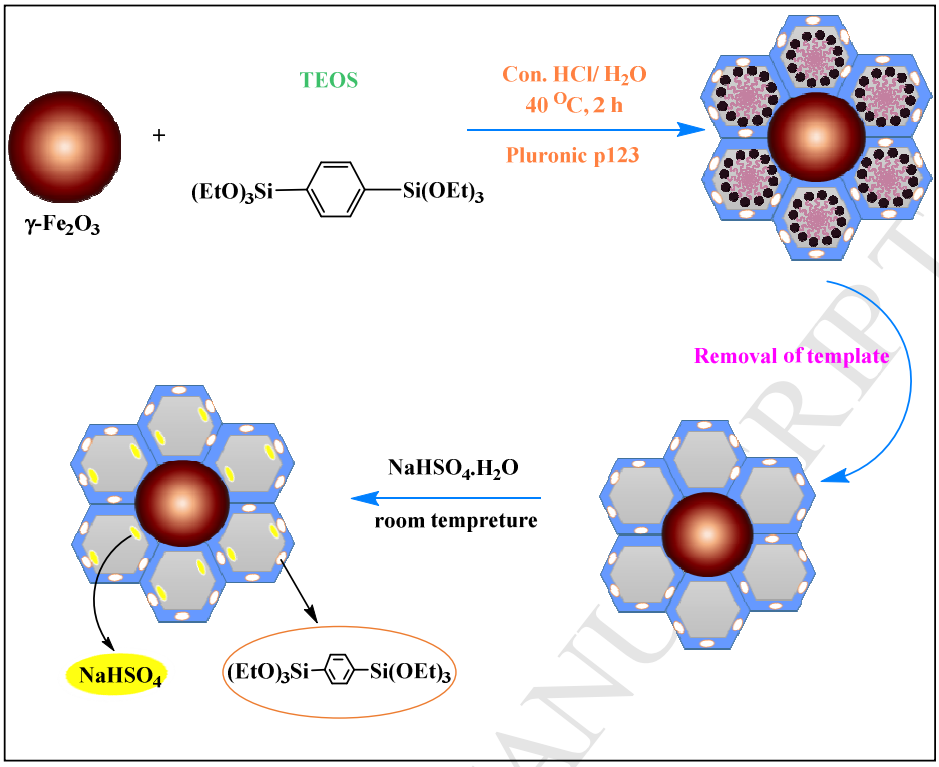

Fig. 1 Preparation of γ-Fe_2O_3@Ph-PMO-$NaHSO_4$.

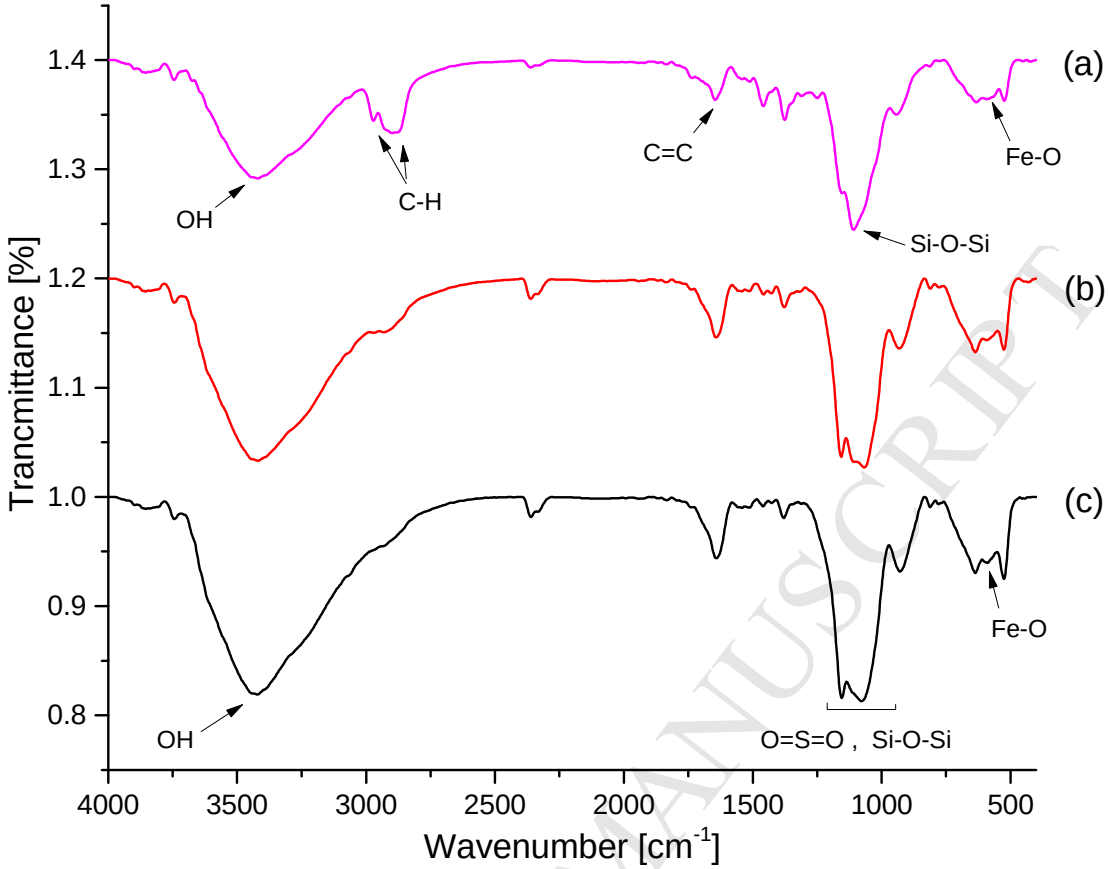

Fig. 2 The FT-IR spectra of γ-Fe_2O_3@Ph-PMO, before removal of the template (a), γ-Fe_2O_3@Ph-PMO, after removal of the template (b) and γ-Fe_2O_3@Ph-PMO-$NaHSO_4$ (c).

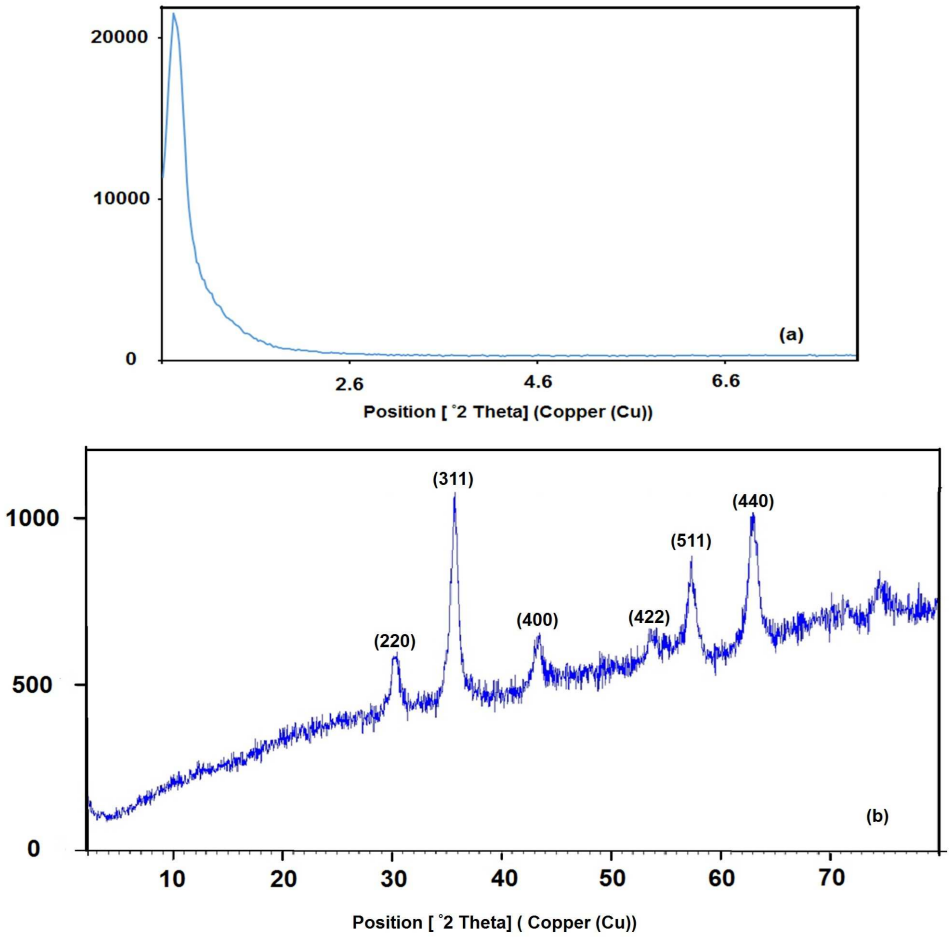

Fig. 3 The XRD pattern of γ-Fe_2O_3@Ph-PMO after removal of the template in low angle (a) and wide angle (b).

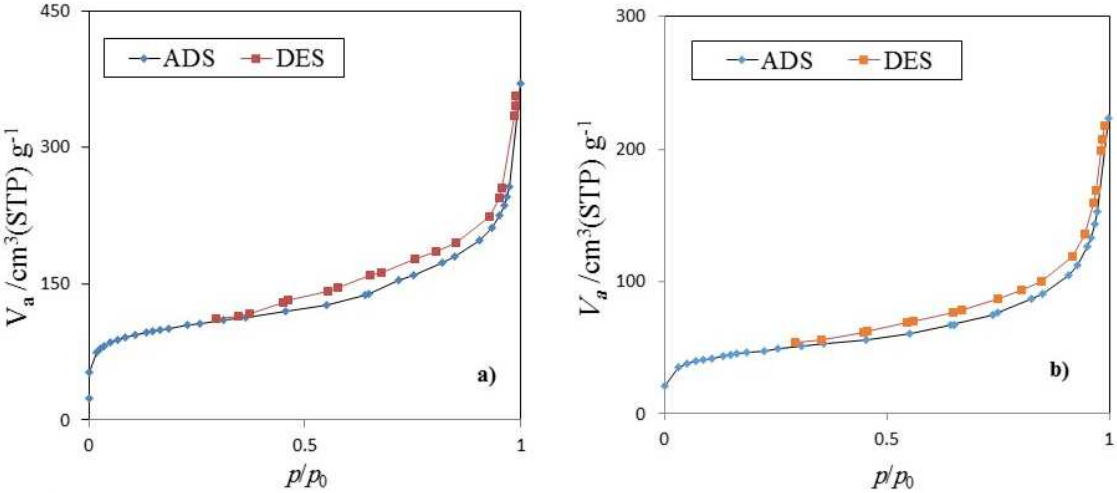

Fig. 4 N_2 adsorption-desorption of γ-Fe_2O_3@Ph-PMO (a), and γ-Fe_2O_3@Ph-PMO-$NaHSO_4$ (b).

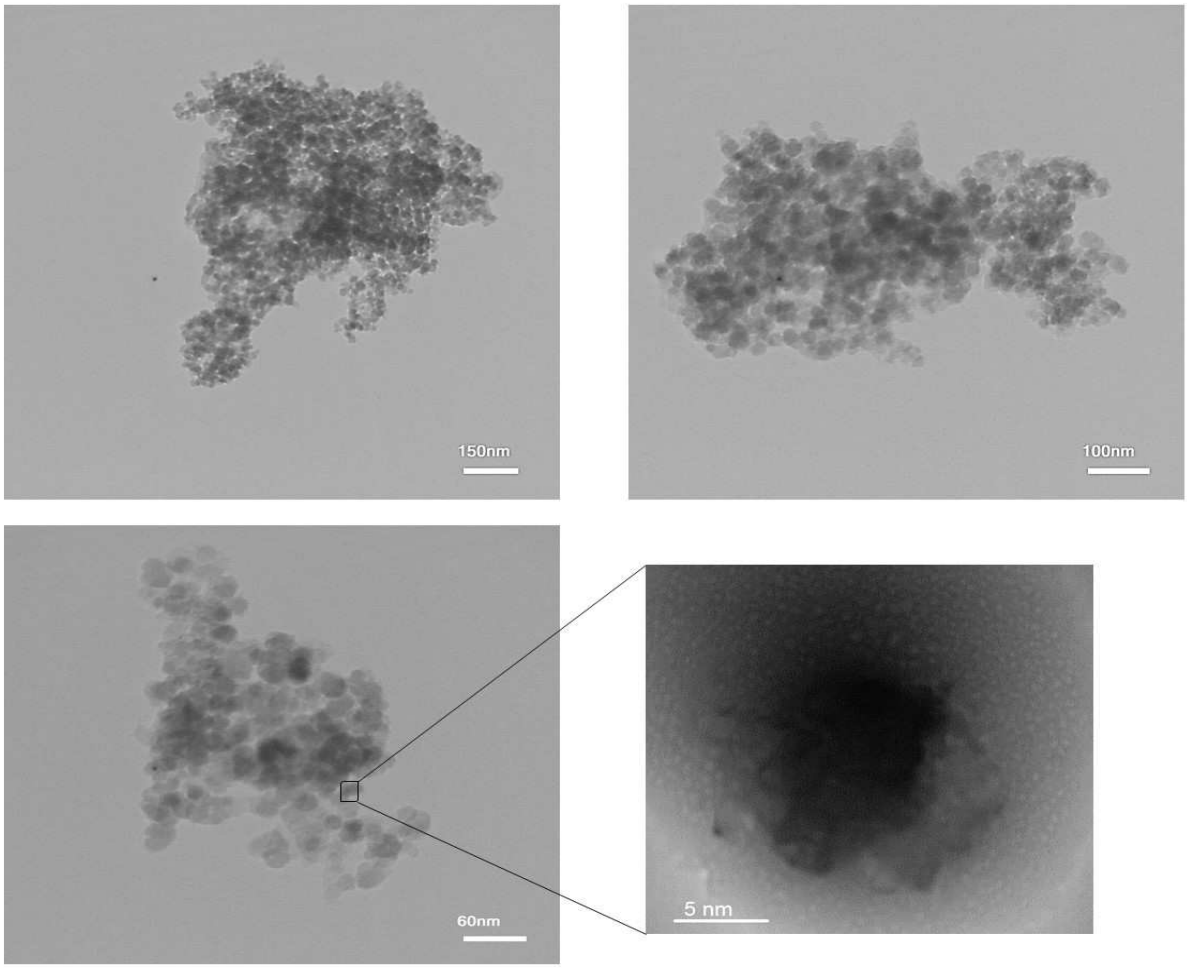

Fig. 5 The TEM images of γ-Fe_2O_3@Ph-PMO-$NaHSO_4$.

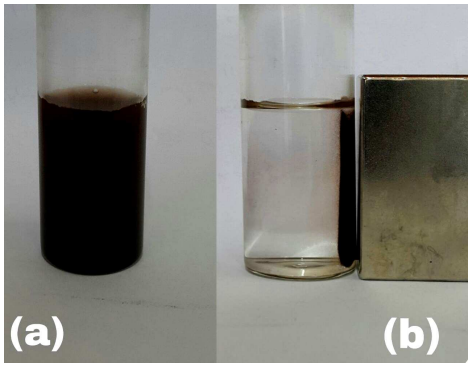

Fig. 6 Photographs of an aqueous suspension of γ-Fe_2O_3@Ph-PMO-$NaHSO_4$ before (a) and after (b) magnetic capture.

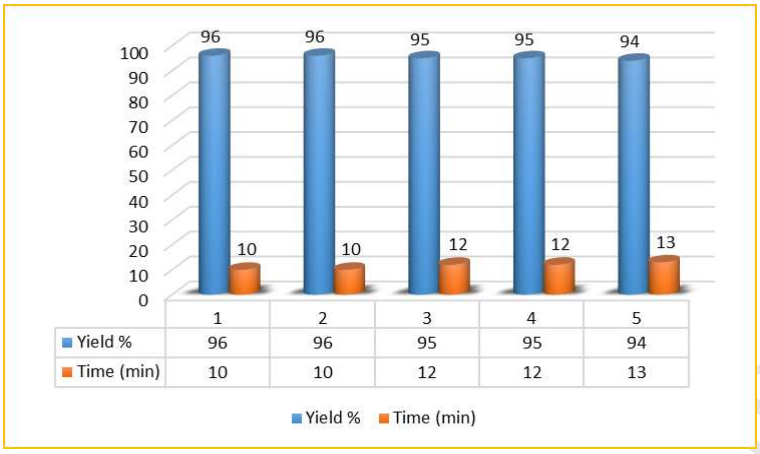

Fig. 7 Reusability of γ-Fe_2O_3@Ph-PMO-$NaHSO_4$ in the synthesis of 9-(4-chlorophenyl)-6,6-dimethyl-5,6,7,9-tetrahydro-[1,2,4]triazolo[5,1-*b*]quinazolin-8(4*H*)-one (6b).

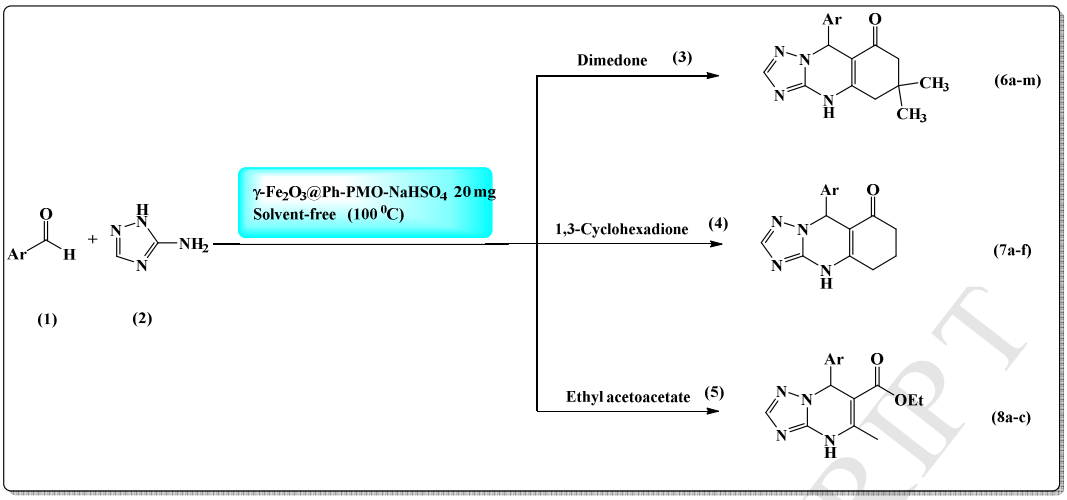

Scheme 1 Synthesis of [1,2,4] triazolo quinazolinone/pyrimidine derivatives catalyzed by γ-Fe_2O_3@Ph-PMO-$NaHSO_4$ under solvent-free condition**.**

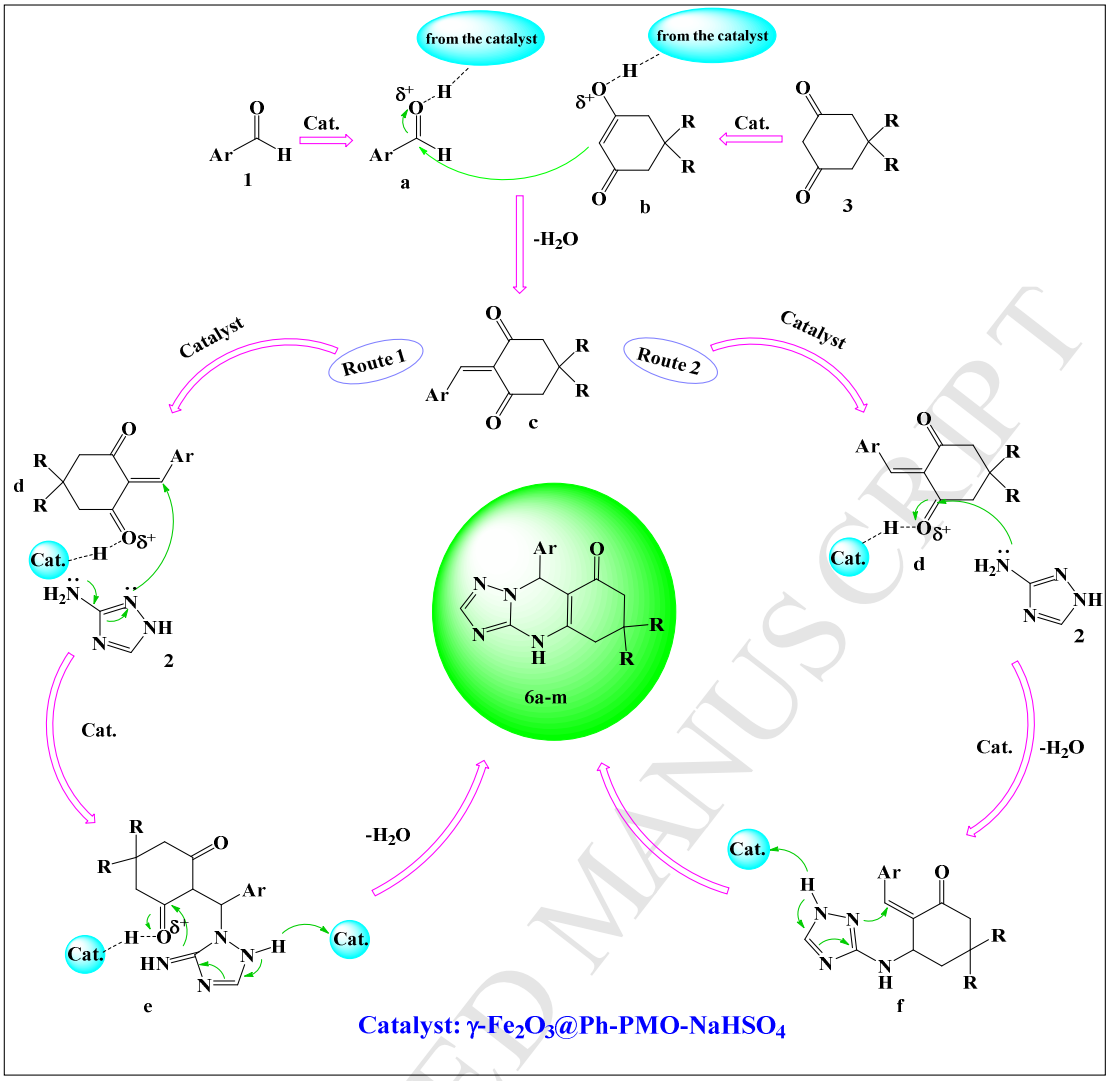

Scheme 2 Plausible mechanism for the preparation of [1,2,4]-triazolo-quinazolinone derivatives in the presence of γ-Fe_2O_3@Ph-PMO-$NaHSO_4$.

Table 1. Structural parameters of the synthesized γ-Fe_2O_3@Ph-PMO, and γ-Fe_2O_3@Ph-PMO-$NaHSO_4$.

	S_{BET} ($m^2.g^{-1}$)	V(cm^3.g)
γ-Fe_2O_3@Ph-PMO	357.83	0.5154
γ-Fe_2O_3@Ph-PMO-$NaHSO_4$	163.5	0.3093

S_{BET}: specific surface area; V: total pore volume at relative pressure 0.99

Table 2. Optimization of the amount of the catalyst, temperature and solvent in the synthesis of [1,2,4]triazolo quinazolinone derivative of 4-chlorobenzaldehyde.

Entry	Amount of the catalyst (g)	Solvent	Temp. (^oC)	Time (min)	Conversion (Yield %)[a]
1	0.02	CH_2Cl_2	r.t.	120	Trace
2	0.02	CH_2C_{l2}	Reflux	120	Trace
3	0.02	CH_3CN	r.t.	120	Trace
4	0.02	CH_3CN	Reflux	120	Trace
5	0.02	H_2O	r.t.	120	Not completed
6	0.02	H_2O	Reflux	120	Not completed
7	0.02	C_2H_5OH	Reflux	80	100(75)
8	0.02	C_2H_5OH : H_2O (1:1)	Reflux	90	100(70)
9	0.01	---	100	25	100(92)
10	0.02	---	100	10	100(96)
11	0.03	---	100	20	100(90)
12	0.02[b]	---	100	120	Trace
13	0.02[c]	---	100	120	Not completed

[a] Isolated yields.
[b] the used catalyst in this procedure was γ-Fe_2O_3@Ph-PMO
[c] the used catalyst in this procedure was $NaHSO_4$

Table 3. Preparation of [1,2,4]triazolo quinazolinone/pyrimidine derivatives using γ-Fe_2O_3@Ph-PMO-$NaHSO_4$ as the catalyst**.**

Entry	Aldehyde	Product		Time (min)	Yield (%)[a]	M.P. (°C) Found	M.P. (°C) Reported	[Ref.]
1	C_6H_5CHO	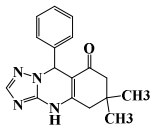	6a	25	93	248-250	250-252	[17]
2	4-ClC_6H_4CHO	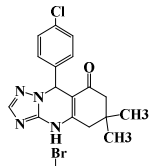	6b	10	96	294-296	303-305	[20]
3	4-BrC_6H_4CHO	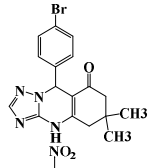	6c	15	94	283-285	284-288	[20]
4	4-$NO_2C_6H_4CHO$	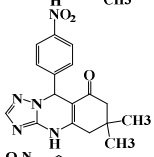	6d	35	90	290-294	307-309	[17]
5	3-$NO_2C_6H_4CHO$	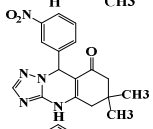	6e	30	90	265-267	266-269	[19]
6	2-$NO_2C_6H_4CHO$	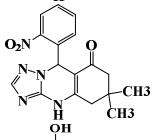	6f	25	91	288-290	290-292	[36]
7	4-OHC_6H_4CHO	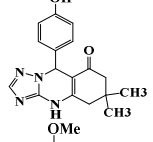	6g	35	90	>300	>300	[19]
8	4-$MeOC_6H_4CHO$	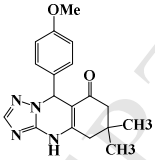	6h	40	90	224-225	222-224	[17]
9	3-$MeOC_6H_4CHO$	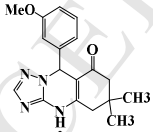	6i	35	93	>300	>300	[37]
10	2-$MeOC_6H_4CHO$	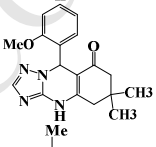	6j	20	93	242-244	240-243	[36]
11	4-MeC_6H_4CHO	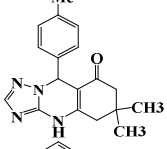	6k	30	90	260-264	264-269	[20]
12	2-MeC_6H_4CHO	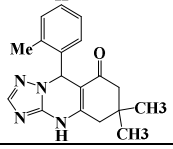	6l	16	92	293-295	295-299	[37]

13	2-Naphthaldehyde	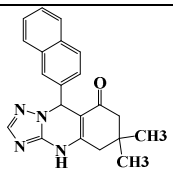	6m	30	96	285-287	287-290	[19]
14	C_6H_5CHO	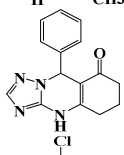	7a	30	90	296-299	296-299	[37]
15	$4\text{-}ClC_6H_4CHO$	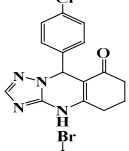	7b	25	89	293-295	294-296	[37]
16	$4\text{-}BrC_6H_4CHO$	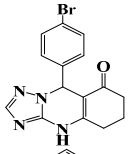	7c	30	90	>300	306-308	[37]
17	$2\text{-}NO_2C_6H_4CHO$	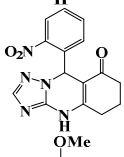	7d	40	89	>300	300-304	[37]
18	$4\text{-}MeOC_6H_4CHO$	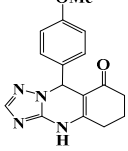	7e	35	90	>300	306-308	[37]
19	$3\text{-}NO_2C_6H_4CHO$	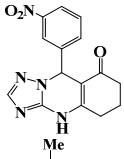	7f	35	89	293-297	292-296	[37]
20	$4\text{-}MeC_6H_4CHO$	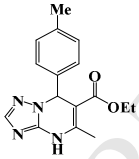	8a	40	90	238-242	246-248	[21]
21	4-NO_2OC6H4CHO	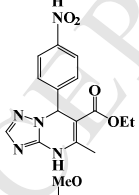	8b	30	87	257-260	263-264	[21]
22	$4\text{-}MeOC_6H_4CHO$	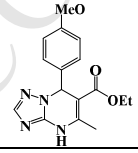	8c	24	85	232-236	220-223	[21]

[a] Isolated yields

Table 4. Catalytic activity and reaction conditions comparison of γ-Fe_2O_3@Ph-PMO-$NaHSO_4$ with other reported catalysts.

Entry	Product	Catalyst	Amount	Condition	Time (min)	Yield (%)	TOF (S^{-1})[a]	[Ref.]
1		---	---	DMF/ Reflux.	30	65	---	[17]
2		---	---	Solvent free/ 110 °C	300	87	---	[38]
3		$H_6P_2W_{18}O_{62}.H_2O$	(0.01 mol)	CH_3CN/ Reflux	30	97	0.001	[19]
4		Sulfamic acid	(0.005 mol)	CH_3CN/ 80 °C	35	95	0.09	[20]
5	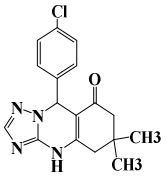 (6b)	Iodine	(0.1 mol)	H_2O: CH_3CN/ Reflux	10	96.1	0.006	[37]
6		p-Toluenesulfonic acid	(0.15 mol)	CH_3CN/ 40-50 °C	10	96	0.0062	[22]
7		Acetic acid	(0.087 mol)	Solvent free/ 60 °C	30	85	0.009	[23]
8		SBA-Pr-SO_3H	0.05 g	Solvent free / 100 °C	5	90	6	[25]
9		Nano-SiO_2	0.15 mol	CH3CN / r.t.	10	94	0.017	[24]
10		Nafion-H®	0.06 g	PEG-400 / 50 °C	35	94	0.746	[39]
11		γ-Fe_2O_3@Ph-PMO-$NaHSO_4$	0.02 g	Solvent free / 100 °C	10	96	8	[This work]

[a] The amounts of catalysts in TOF were calculated in term of gram of catalysts for all mentioned catalysts in the Table.

Highlights:

- Preparation of Immobilized $NaHSO_4$ on core/shell phenylene bridged Periodic mesoporous organosilica magnetic nanoparticles.
- Introduction of a simple method for the preparation of [1,2,4]triazolo quinazolinone/pyrimidine derivatives.
- Easy separation and reusability of the nanocatalyst.